Journal of *Marine Science and Engineering*

MDPI

Article

Balancing Efficiency and Economics in Organic Rankine Cycles with Multistage Turbines for Sustainable Waste Heat Utilization

Sattam Alharbi [1], Nasser Alanazi [2], Maha Alharbi [3], Mamdouh H. Alshammari [1], Apostolos Pesyridis [4] and Fuhaid Alshammari [1,*]

[1] Mechanical Engineering Department, College of Engineering, University of Hail, Hail 2440, Saudi Arabia; sm.alharbi@uoh.edu.sa (S.A.); mah.alshammari@uoh.edu.sa (M.H.A.)
[2] Civil Engineering Department, College of Engineering, University of Hail, Hail 2440, Saudi Arabia; n.alanazi@uoh.edu.sa
[3] Biology Department, College of Science, University of Hail, Hail 2440, Saudi Arabia; moh.alharbi@uoh.edu.sa
[4] College of Engineering & Technology, University of Doha for Science & Technology, Doha P. O. Box 24449, Qatar; apostolos.pesyridis@udst.edu.qa
* Correspondence: fu.alshammari@uoh.edu.sa

Abstract

Thermal energy rejected through exhaust gases and cooling systems in marine propulsion units and conventional power plants represents a significant yet underutilized opportunity for improving energy efficiency and reducing carbon emissions. The Organic Rankine Cycle (ORC) has emerged as an effective technology for converting such waste heat into useful power using organic working fluids with favorable thermophysical properties. This study presents a comprehensive thermodynamic, economic, and exergo-economic evaluation of an ORC system incorporating single-stage and multistage turbine arrangements, using R245fa, R123, and R365mfc as working fluids. A validated cycle model is coupled with key economic indicators, including Net Present Value (NPV), Levelized Cost of Electricity (LCOE), and payback period, together with a simplified exergo-economic framework based on exergy destruction costs. The results demonstrate that implementing ORC-based waste heat recovery significantly enhances overall system performance by converting rejected thermal energy into electricity and improving thermal efficiency. Multistage turbine configurations further strengthen performance, increasing net power output and efficiency, with the multistage R245fa system generating more than 530,000 kWh annually. Economically, the single-stage R245fa configuration achieves the lowest LCOE (0.021 USD/kWh) and the shortest payback period, below eight years. Exergo-economic analysis shows that multistage turbines can reduce exergy destruction costs by more than 80%, with benefits becoming pronounced at heat source temperatures above 170 °C.

Keywords: waste heat recovery (WHR); organic Rankine cycle (ORC); multistage turbine; economic model; marine; power plant

Check for updates

Academic Editors: Kai Wang and Nikos Themelis

Received: 24 December 2025
Revised: 24 January 2026
Accepted: 26 January 2026
Published: 27 January 2026

Copyright: © 2026 by the authors. Licensee MDPI, Basel, Switzerland. This article is an open access article distributed under the terms and conditions of the Creative Commons Attribution (CC BY) license.

1. Introduction

Thermal energy rejected as waste heat, most notably from marine propulsion systems and conventional power plants, constitutes a significant but still underexploited resource for sustainable power generation. In both ship engines and land-based power stations, a considerable portion of the fuel's chemical energy is dissipated through exhaust gases, engine cooling systems, and auxiliary thermal streams [1]. For marine engines, exhaust gas temperatures downstream of turbochargers typically fall within the range of approximately

200–400 °C, while jacket water and charge-air cooling circuits usually operate between 70 and 120 °C [2]. Comparable conditions are observed in conventional power plants, where low-pressure exhaust steam, flue gases, and cooling systems commonly release heat at temperatures below 150 °C. Although such temperature levels are generally unsuitable for conventional steam Rankine cycles, they align well with the operating characteristics of organic working fluids [3].

In this context, the Organic Rankine Cycle (ORC) has gained increasing attention as a practical solution for converting waste heat into useful power [4]. By employing organic fluids with favorable thermophysical properties, ORC systems can operate efficiently at moderate pressures and temperatures. Their relatively compact size, operational flexibility, and ease of integration with existing thermal infrastructure make them particularly attractive for shipboard installations and stationary power-generation applications [5]. Importantly, ORC deployment typically requires minimal modification to the prime mover. By transforming otherwise discarded thermal energy into electricity, ORC systems reduce auxiliary power demand and fuel consumption, thereby contributing to lower greenhouse gas emissions. As a result, ORC-based waste heat recovery enhances overall system efficiency while supporting decarbonization objectives in both maritime and power-generation sectors, with additional benefits in terms of economic performance.

Within an ORC system, the turbine represents a critical component governing overall cycle efficiency, power output, and operational flexibility. For small- to medium-scale applications, single-stage turbines are often preferred due to their compact configuration, mechanical simplicity, and ability to accommodate relatively large enthalpy drops within a single expansion stage [6]. However, under high pressure ratios or variable heat-source conditions, both of which are characteristic of waste heat recovery applications, single-stage turbines may suffer noticeable performance degradation. This deterioration is primarily linked to adverse aerodynamic effects, including shock formation, flow choking at the throat, increased entropy generation, and, in certain cases, partial condensation when dense organic fluids are used. Collectively, these phenomena reduce isentropic efficiency and may also raise concerns regarding long-term turbine reliability.

To address these limitations, multistage turbine configurations have been proposed as a more advanced alternative. By distributing the total expansion across multiple rotor–stator stages, each stage operates at a lower pressure ratio and reduced Mach number, thereby mitigating aerodynamic losses and improving flow stability [7]. Such arrangements also enable improved matching between the thermodynamic properties of the working fluid and the blade loading in each stage. Previous studies have shown that multistage turbines can achieve efficiency improvements exceeding 10%, while simultaneously expanding the operational envelope of ORC systems. Moreover, their lower sensitivity to off-design conditions makes them well-suited for applications in which the magnitude or quality of the heat source varies over time. These advantages, however, come at the cost of increased mechanical complexity, higher manufacturing and maintenance requirements, and more stringent demands on rotor balancing and sealing. Consequently, careful techno-economic evaluation is essential before such configurations can be adopted in practice.

Turbines employed in ORC systems are generally classified as either axial or radial machines [8]. Both configurations rely on the same fundamental energy-conversion mechanism, whereby the working fluid expands through stationary and rotating blade rows, converting thermal energy into mechanical work [9]. In both cases, the stator accelerates and directs the flow toward the rotor, which extracts energy through changes in fluid momentum [10]. Accordingly, similar performance indicators, such as pressure ratio, mass flow rate, isentropic efficiency, and power output, are used to assess axial and radial turbines. Despite these shared principles, the two turbine types differ markedly in terms

of flow orientation, geometric configuration, and suitability for specific applications [11]. Axial turbines feature flow paths predominantly aligned with the axis of rotation, allowing high mass flow rates and making them suitable for applications involving moderate pressure ratios [12]. Radial turbines, by contrast, accommodate flow that enters radially and exits either axially or radially, enabling higher pressure ratios per stage and more compact designs. In addition, radial turbines tend to be more robust and less sensitive to off-design operation, which makes them particularly attractive for small-scale ORC systems and waste heat recovery applications [13]. While axial turbines can achieve higher peak efficiencies under optimized conditions, they typically require multiple stages and tighter manufacturing tolerances to reach comparable pressure ratios. These inherent distinctions result in different trade-offs in terms of size, efficiency, scalability, and system integration within ORC frameworks.

Table 1 summarizes recent developments in engine-ORC integration. Although substantial progress has been made in thermodynamic optimization and aerodynamic design, economic aspects have received comparatively less attention. This gap is non-trivial, as the commercial viability of ORC technology ultimately determines whether such systems can transition from laboratory-scale studies to widespread industrial implementation. While efficiency improvements are essential, investment decisions in real-world applications are largely driven by capital costs, operating expenses, and anticipated financial returns. This consideration is particularly important for multistage radial turbines, where performance gains are achieved at the expense of increased mechanical complexity and cost. In such cases, economic evaluation becomes indispensable. Financial metrics such as the Levelized Cost of Electricity (LCOE), Net Present Value (NPV), and payback period provide critical benchmarks for assessing competitiveness. Given that waste heat recovery projects often operate within narrow economic margins, cost optimization plays a decisive role in ensuring market acceptance. Accordingly, the integration of economic and exergo-economic analyses into ORC research is essential for bridging the gap between technical advancement and industrial deployment, ensuring that proposed solutions are not only efficient but also financially viable.

Table 1. Summary of the recent advancements in WHR–ORC applications.

Ref.	Engine/Heat Source	Application/System	Methodology	Main Findings
[14]	Heavy-lift vessels (marine engines)	Marine propulsion decarbonization	Techno-economic analysis	Methanol-fueled engines showed cost-effective compliance with Fuel EU Maritime regulations.
[15]	Ocean-going cargo ship	Wind-assisted + ORC integration	Thermodynamic modeling	Combined wind propulsion and ORC reduced fuel consumption by up to 21%.
[16]	Commercial ships (EU MRV data)	Energy efficiency assessment	Data-driven analysis	Efficiency improvements and inconsistencies between EU MRV and IMO datasets.
[17]	Two-stroke marine diesel engine	ORC-based waste heat recovery	Exergy analysis	Proper working fluid improved power output and exergy efficiency.
[18]	Conventional power plant	Combined-cycle optimization	Thermodynamic and environmental analysis	ORC integration reduced CO_2 emissions by over 7.5%.
[19]	Ocean thermal energy (OTEC platform)	Marine ORC power generation	Experimental study	Demonstrated stable grid-connected operation with ~2.5% thermal efficiency.
[20]	LNG carrier engine + BOG	Hydrogen production via ORC	Thermo-economic comparison	SOEC coupled with ORC achieved the lowest hydrogen cost.

Table 1. *Cont.*

Ref.	Engine/Heat Source	Application/System	Methodology	Main Findings
[21]	Engines, industrial WH, renewables	ORC technology review	Comprehensive literature review	Two-stage ORCs improved thermal efficiency by up to 20%.
[3]	Gas turbine power plant (Baghdad)	ORC integration in power plants	Exergo-economic analysis	Brayton–ORC configuration raised overall efficiency above 44%.
[22]	Buoy maintenance vessel	Hybrid marine propulsion	Real-sea operational data	Hybrid electric propulsion achieved 2.02% fuel and CO_2 reductions.
[23]	Industrial waste heat and thermal pollution sources	General ORC technology overview	Comprehensive review	Identified ORC as a key technology for electricity generation.
[24]	Geothermal energy systems	Binary ORC power plants	Thermodynamic optimization	Demonstrated that optimized binary ORC configurations significantly enhance efficiency and power output.
[25]	Thermal power plants	Power plant operational enhancement	Control strategy and system analysis	Showed that cascade Rankine cycle integration with advanced feedwater control improves thermal efficiency.

A review of the existing literature reveals that while extensive efforts have been devoted to thermodynamic modeling and aerodynamic optimization, comprehensive economic evaluations of multistage radial turbine ORCs remain scarce. This research seeks to address this gap by developing a detailed thermodynamic, economic, and exergo-economic framework for ORC systems incorporating multistage turbines. Specifically, the study evaluates the influence of turbine configuration and working fluid choice on net power generation, thermal efficiency, payback period, and unit exergy cost. Four turbine configurations are investigated, namely, single-stage axial turbine, single-stage radial turbine, multistage axial turbine, and multistage radial turbine. By coupling performance simulations with financial analysis, the study provides valuable insights for technology developers, investors, and policymakers, thereby supporting the design of cost-effective, low-carbon power generation systems. This paper is organized as follows: Section 2 presents the system description and modeling methodology; Section 3 discusses the thermodynamic, economic, and exergo-economic results; Section 4 concludes the study with key findings and directions for future work.

2. System Modeling

Figure 1 presents a typical ORC system considering a thermal energy source, and the ORC system, including the multistage turbine. The fundamental aim of the ORC system is to harness heat sources, such as industrial waste heat and marine waste heat, and convert them into useful power. By employing organic fluids with favorable boiling characteristics, ORC systems can efficiently operate at lower pressures and temperatures than conventional steam Rankine cycles [5]. This enables the recovery of energy that would otherwise be discarded, thereby improving overall energy efficiency, reducing greenhouse gas emissions, and supporting sustainable power generation [26].

The mathematical framework developed for this study combines thermodynamic, economic, and exergo-economic models to evaluate the performance of the ORC configurations. The thermodynamic model is based on steady-state assumptions, with negligible pressure losses in the heat exchangers. As shown in Figure 1, the working fluid undergoes four main processes in a closed loop: evaporation, expansion, condensation, and pressurization, corresponding to the evaporator (1-2), turbine (2-3), condenser (3-4), and pump (4-1). In the cycle, the liquid working fluid is first pressurized by a pump and then

directed to the evaporator, where it absorbs heat from the waste heat source and undergoes vaporization. The resulting high-pressure vapor expands through the turbine, converting thermal energy into mechanical work that can be used to generate electricity. After expansion, the low-pressure vapor exits the turbine and flows into the condenser, where it rejects heat to a cooling medium and condenses back into a liquid state. The condensed fluid is then pumped back to the evaporator, completing the cycle. The thermophysical properties of the organic fluids are evaluated using REFPROP 9.0 [27] to ensure accurate prediction of real-gas behavior. The economic model is constructed using a discounted cash flow framework to determine the financial feasibility of each configuration.

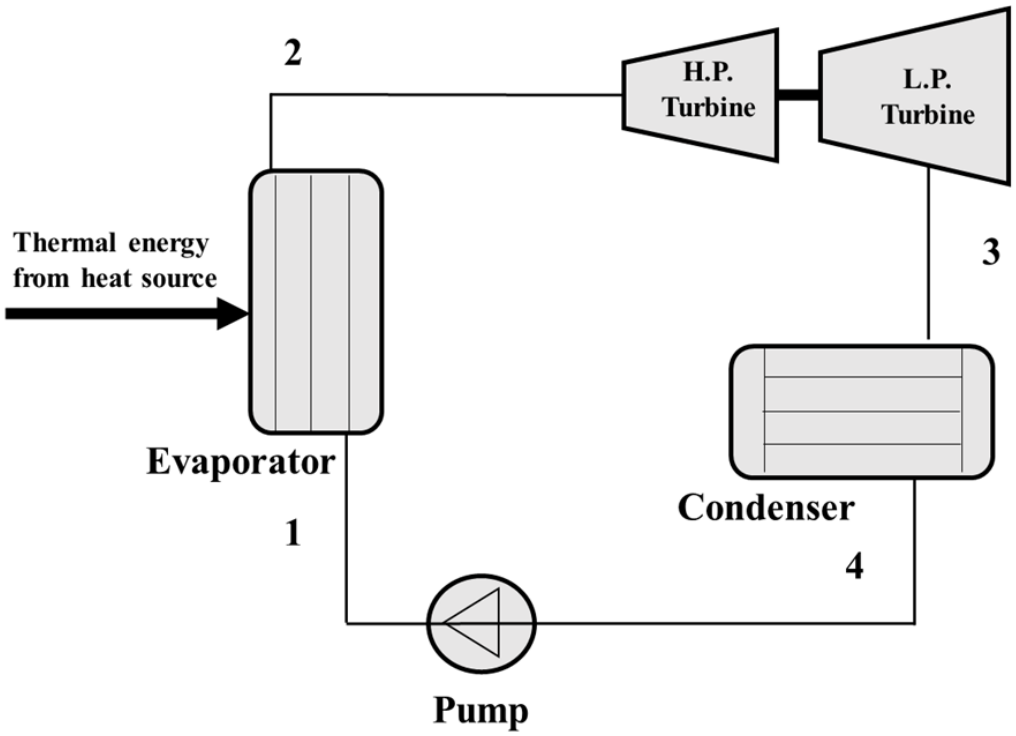


Figure 1. Structure of the ORC system considering a multistage turbine. For a single-stage configuration, only one turbine stage is employed.

The primary aim of employing multistage turbines in ORC systems is to enhance efficiency and operational stability under high pressure ratios or large enthalpy drops. By distributing the expansion process across multiple stages, each stage operates at lower Mach numbers and reduced pressure ratios, thereby minimizing aerodynamic losses such as shock formation and entropy generation. This approach enhances isentropic efficiency, improves adaptability to variable heat source conditions, and ensures better thermodynamic matching with the properties of organic working fluids, ultimately leading to more reliable and cost-effective energy conversion. Table 2 summarizes the representative range of operating conditions considered in the present study. Figure 2 outlines the sequential modeling framework, starting from the definition of operating conditions and working-fluid selection, followed by thermodynamic cycle simulation, turbine performance evaluation, and subsequent economic and exergo-economic analyses.

Table 2. Representative range of operating conditions for ORC modeling.

Parameter	Unit	Range
Marine exhaust gas, power plant flue gas, jacket water	°C	120–200

Table 2. *Cont.*

Parameter	Unit	Range
Organic fluid vaporization	MPa	1.2–3.5
Cooling water	°C	30–45
Saturation pressure	MPa	0.15–0.35
Pressure ratio across the turbine	-	4–12
Mass flow rate	Kg/s	0.1–1.5
Turbine inlet temperature	°C	110–190

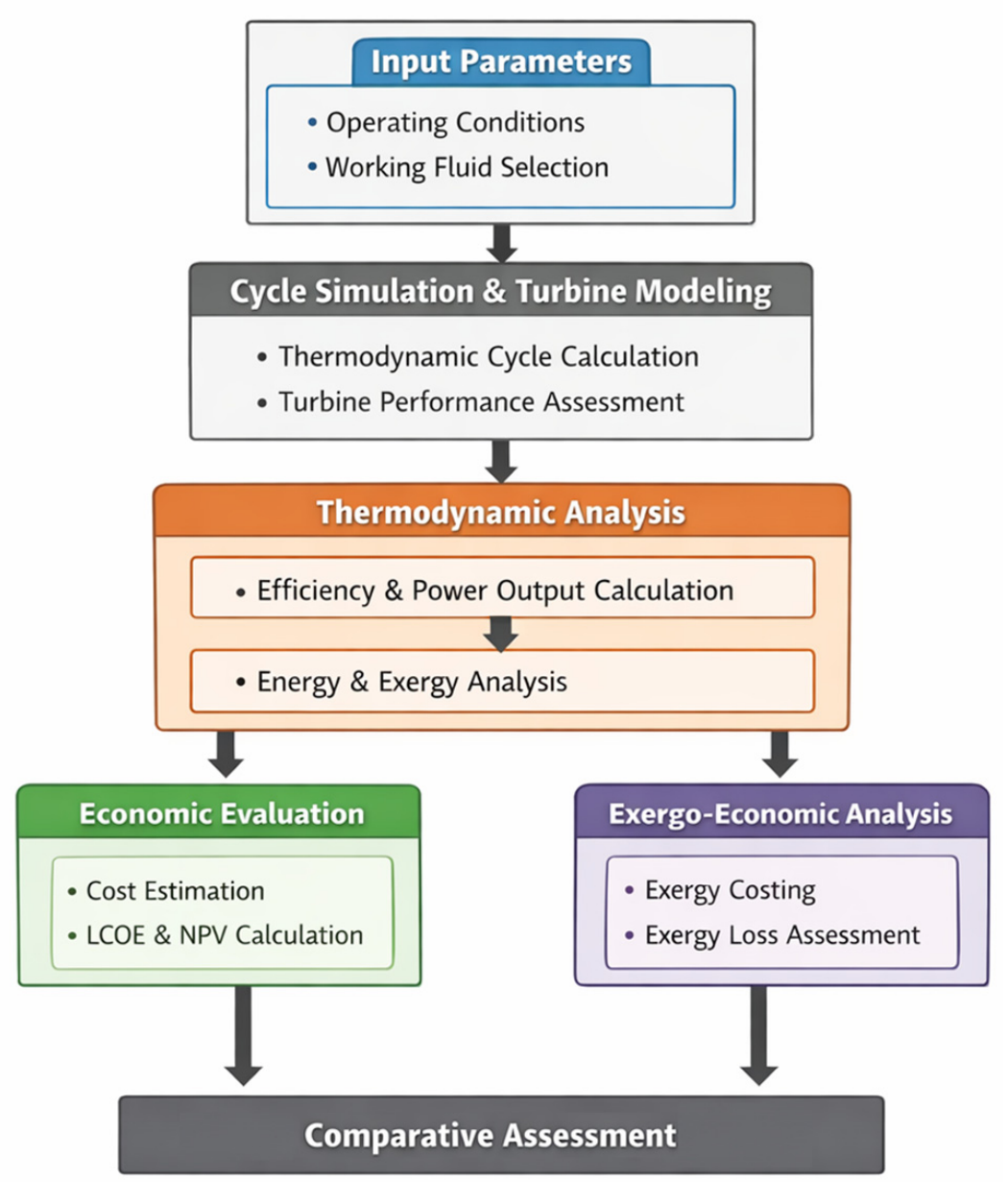


Figure 2. Schematic illustration of the overall modeling framework adopted in this study.

2.1. Thermodynamic Model

The ORC configuration considered in this study consists of an evaporator, a turbine, a condenser, and a pump arranged in a closed-loop layout. Thermal energy supplied to the evaporator raises the working fluid to the vapor state, as illustrated in Figure 1. The resulting vapor expands through the turbine to produce mechanical power, after which it is condensed and returned to the evaporator inlet by the pump, thereby completing the cycle. The energy balance and thermodynamic relations are detailed in the study [28]. Table 3

presents a summary of the main equations used for the modeling of the ORC system. $\dot{m}_{wf}$ and h are the mass flow rate and the enthalpy of the fluid.

Table 3. Summary of ORC mathematical modeling.

Eqn.	Eqn. #	Notes
$\dot{Q}_{evap} = \dot{m}_{wf}(h_2 - h_1)$	(1)	The amount of heat absorbed from the heat source by the working fluid.
$\dot{W}_{turb} = \dot{m}_{wf}(h_2 - h_3)$	(2)	The power output produced by the turbine.
$\dot{Q}_{cond} = \dot{m}_{wf}(h_3 - h_4)$	(3)	The amount of heat rejected in the condenser to condense the vapor.
$\dot{W}_{pump} = \dot{m}_{wf}(h_1 - h_4)$	(4)	The power input to the pump raises the fluid pressure from condenser pressure to evaporator pressure.

It should be noted that the energy balance equations and thermodynamic relations employed in this study are not newly developed but are adopted from our previously published work [28]. In Ref. [28], the same ORC modeling framework, including mass and energy conservation, turbine and pump performance formulations, and working-fluid property evaluation using REFPROP 9.0, was rigorously validated against published experimental and numerical results for organic Rankine cycle systems. A good agreement was reported in terms of net power output, thermal efficiency, and sensitivity to operating conditions. The present study, therefore, builds upon this previously validated thermodynamic model and extends its application to a comparative assessment of turbine configurations and techno-economic performance, rather than re-validating the underlying formulation.

2.2. Turbine Configurations

Figure 3 illustrates the turbine configurations examined in this work. The radial turbine consists of a volute, stator, and rotor as its principal components. The volute collects the working vapor and distributes it circumferentially toward the stator inlet. As the flow passes through the stator, its direction is adjusted to match the rotor inlet angle, accompanied by a small pressure drop. The vapor then expands through the rotor blades, where its thermal energy is converted into mechanical power. Although axial turbines rely on the same fundamental energy conversion process, they differ in their flow admission strategy. In axial configurations, the working fluid enters the stator directly along the turbine axis, removing the need for a volute and resulting in a simpler inlet layout.

Turbine performance is evaluated using a stage-by-stage thermodynamic modeling approach. Isentropic expansion is adopted as the ideal reference process, while real-gas effects and irreversibilities are incorporated using isentropic efficiency. Both axial and radial turbines are analyzed under steady-state conditions. For multistage configurations, the total pressure ratio is evenly divided among the stages, allowing each stage to be treated using the same thermodynamic formulation applied to the first stage.

The flow stations employed in the analysis are also indicated in Figure 3. For the radial turbine, stations 2 and 3 represent the overall turbine inlet and outlet, respectively. Locations a, b, and c correspond to the stator inlet, stator exit (which also serves as the rotor inlet), and rotor exit of the first stage. The second stage is defined by stations d, e, and 3, which denote the inlet and outlet of its individual components. In the axial turbine layout, station 2 identifies the stator inlet, point a represents the stator exit and rotor inlet, and point b denotes the rotor exit.

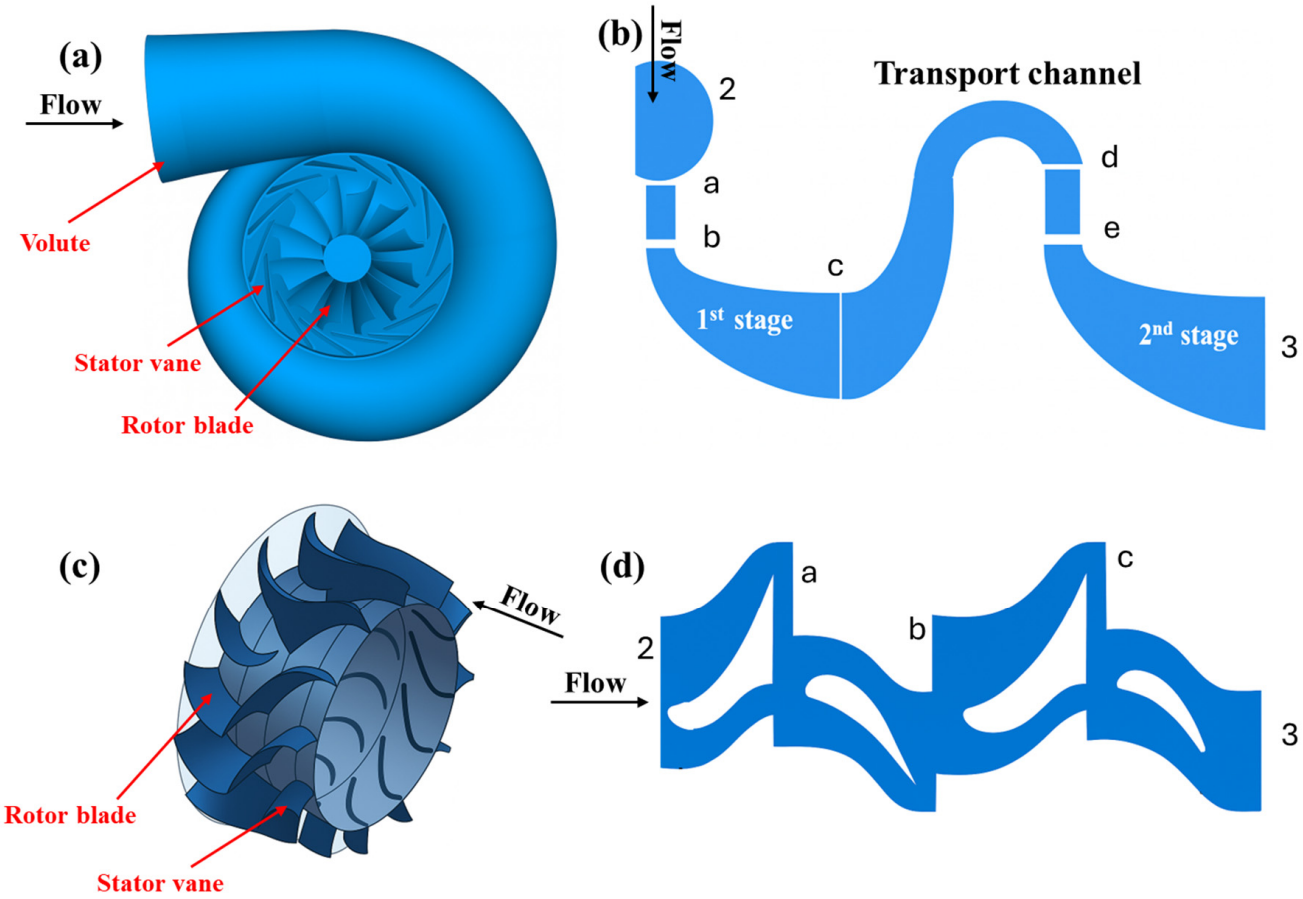


Figure 3. Visualization of single and multistage radial turbines (**a**,**b**), and single and multistage axial turbines (**c**,**d**).

It should be noted that the aim of this study is to evaluate and compare the performance characteristics of different turbine configurations, rather than to address detailed geometric design or blade optimization for either turbine type.

2.3. Working Fluids

This study examines three organic working fluids—R245fa, R123, and R365mfc—selected to enable a balanced comparison of thermodynamic performance, expansion behavior, and economic implications in low- to medium-temperature Organic Rankine Cycle applications. These fluids have been extensively reported in the ORC literature for waste heat recovery from industrial processes, marine propulsion systems, and conventional power plants, primarily due to their appropriate boiling temperatures, moderate critical properties, and favorable saturation pressure levels within the operating temperature range considered.

R245fa is widely adopted as a reference working fluid in ORC studies, owing to its reliable performance, comparatively high cycle efficiency, and proven compatibility with radial inflow turbines. R123, which features a higher critical temperature, is particularly suitable for applications involving higher-temperature heat sources and can offer improved expansion efficiency under elevated turbine inlet conditions. By contrast, R365mfc possesses a higher molecular weight and vapor density, characteristics that support compact turbomachinery designs but also increase sensitivity to expansion matching and irreversibility effects during turbine operation. Taken together, the selected working fluids provide a representative basis for assessing the influence of thermophysical properties on turbine staging, cycle efficiency, and economic performance. This selection ensures that the analysis remains closely aligned with realistic waste heat recovery scenarios encountered in both

maritime and stationary power-generation systems. The key physical properties of the three working fluids are summarized in Table 4.

Table 4. Summary of the thermophysical properties of the investigated fluids.

Property	R365mfc	R123	R245fa
Molecular weight	148.07	152.93	134.05
Normal boiling point	40.2	27.8	15.3
Critical temperature	186.9	183.7	154
Critical pressure	3.27	3.67	3.65
Latent heat of vaporization (NBP)	~183	~167	~196
Ozone depletion potential	0	0.012	0
Global warming potential (100 yr)	~794	~77	~1030

2.4. Economic Model

To assess the economic feasibility of each ORC configuration, a discounted cash flow method is used. Capital and operational expenditures are modeled to determine economic viability. The capital expenditure (CAPEX) is calculated from estimated turbines and component costs. The operational expenditure (OPEX) is taken as a percentage of CAPEX. Net present value (NPV), levelized cost of electricity (LCOE), and payback period are calculated using standard discounted cash flow methods.

CAPEX refers to the total upfront investment required to purchase, install, and commission the major components of a system. It represents the fixed, non-recurring costs needed to bring the system into operational status. In this study, CAPEX is estimated based on equipment cost functions and scaled according to turbine complexity (e.g., number of stages, blade number) as shown in Equation (5). The overall cost is calculated by adding up the expenses of all the main ORC components—such as the turbine, evaporator, condenser, pump, and auxiliary systems. These costs are estimated using scaling functions that link equipment size (for example, heat duty, mass flow rate, or pressure ratio) to price. After that, a correction factor is applied to cover installation, commissioning, and system complexity, including aspects such as the number of turbine stages. The OPEX is modeled as a percentage of the CAPEX, following a common practice in early-stage techno-economic assessments of ORC systems. An OPEX range of 2.8–3.0% of CAPEX is adopted to represent routine operation, inspection, and maintenance activities, consistent with values reported for small- to medium-scale ORC installations in the literature [29,30]. Higher OPEX ratios are assigned to multistage turbine configurations to account for increased mechanical complexity, inspection requirements, and maintenance effort. This formulation is intended for comparative evaluation of different ORC configurations under consistent assumptions, rather than for detailed project-level cost forecasting, which would require finalized mechanical designs and vendor-specific data.

$$CAPEX = C_{turbine} + C_{heat\ exchangers} + C_{pump} + C_{installation} \quad (5)$$

Annual operating cost is modeled as a fixed percentage of CAPEX as shown in Equation (6). α ranges from 2.8 to 3.0% depending on configuration. The lower bound of the range is applied to simpler (single-stage) configurations, while the upper bound is assigned to more complex (multistage) configurations to account for additional inspection, sealing, balancing, and maintenance requirements.

$$OPEX_{annual} = \alpha\ CAPEX \quad (6)$$

Annual revenue, which is expressed in Equation (7), is the total amount of money earned in one year by selling the electricity produced by the ORC system. E_{annual} and

$P_{electricity}$ are the annual electricity output of the ORC system (measured in kWh/year), and the selling price of electricity in USD/kWh, respectively.

$$Revenue_{annual} = E_{annual}\, P_{electricity} \tag{7}$$

Levelized Cost of Electricity represents the average cost to generate one kilowatt-hour (kWh) of electricity over the entire lifetime of the ORC system, accounting for both capital and operating costs. It is expressed in Equation (8). r is the discount rate and N is the system lifetime (20 years).

$$LCOE = \frac{CAPEX + \sum_{n=1}^{N} \frac{OPEX_n}{(1+r)^n}}{\sum_{n=1}^{N} \frac{E_{annual,n}}{(1+r)^n}} \tag{8}$$

The net present value (NPV) of the ORC project over its lifetime, expressed in today's money, is shown in Equation (9).

$$NPV = \sum_{n=1}^{N} \frac{Revenue_n - OPEX_n}{(1+r)^n} - CAPEX \tag{9}$$

The number of years it takes for the accumulated electricity revenues to equal capital investment is shown in Equation (10).

$$Payback = \frac{CAPEX}{Revenue_{annual} - OPEX_{annual}} \tag{10}$$

2.5. Exergo-Economic Model

To link irreversibility with cost, a simplified exergo-economic penalty function based on lost work potential is used. Exergy destruction cost is modeled based on the inefficiency gap from a 15% benchmark thermal efficiency. Annual heat input is estimated from net power and efficiency, and the cost of exergy loss is computed accordingly.

First, the total annual heat input is estimated as shown in Equation (11). It represents the total thermal energy supplied to the ORC cycle annually. η_{th} is the thermal efficiency of the system.

$$Q_{in,annual} = \frac{E_{annual}}{\eta_{th}} \tag{11}$$

Exergy destruction cost, which represents the cost penalty reflecting the thermodynamic irreversibilities in the ORC system, is obtained using Equation (12), where 0.01 USD is assigned per 1% loss in efficiency per kWh. The loss-cost coefficient is introduced as a scaling parameter for comparative exergo-economic assessment and does not represent a fixed or market-derived unit cost; its uniform application ensures that relative performance trends remain unaffected by its absolute value.

$$C_{ex,annual} = (15 - \eta_{th}) \cdot 0.01 \cdot Q_{in,annual} \tag{12}$$

Unit Exergy Cost, which represents the cost of exergy destruction per unit of useful electrical output $\left[\frac{USD}{kWh_e}\right]$ is expressed in Equation (13). This parameter reflects the economic cost of exergy destruction per unit of useful electrical output. Lower values indicate more efficient and cost-effective thermodynamic conversion.

$$Unit\ Exergy\ Cost = \frac{C_{ex,annual}}{E_{annual}} \tag{13}$$

3. Results and Discussions

The results are obtained through a systematic computational procedure based on the thermodynamic, economic, and exergo-economic models described in Section 2. First, the operating conditions are defined, including heat source temperature, condenser temperature, turbine inlet pressure, and working-fluid properties obtained from REFPROP 9.0. For each working fluid and turbine configuration (single-stage and multistage), the ORC thermodynamic cycle is solved using mass and energy balance equations to determine state points, turbine work, pump work, heat input, net power output, and thermal efficiency. The turbine performance is evaluated using isentropic efficiency values adopted from the literature and applied consistently across all cases. The thermodynamic outputs are then used as inputs for the economic model, where CAPEX, OPEX, annual electricity generation, and electricity selling price are employed to calculate LCOE, NPV, and payback period. Subsequently, exergo-economic indicators are derived using the benchmark thermal efficiency and loss-cost coefficient defined in Section 2.5.

3.1. Thermodynamic Performance Overview

Figure 4 illustrates the annual electricity generation of six ORC configurations, combining three working fluids (R245fa, R123, R365mfc) with either single-stage or multistage radial turbines. The results demonstrate that multistage configurations typically deliver better performance than single-stage designs across all fluids, with improvements in net electricity output ranging from approximately 5% to 8%. Among the evaluated cases, the multistage R245fa configuration exhibits the highest performance, delivering more than 530,000 kWh annually. This outcome highlights both the advantageous thermodynamic properties of R245fa and the efficiency gains associated with multistage expansion. R123 also achieves competitive results, though its output remains slightly below that of R245fa. By contrast, R365mfc consistently yields the lowest performance, with particularly notable underperformance in the multistage configuration. Interestingly, the multistage R365mfc system generates less electricity than its single-stage counterpart, a result that may be attributed to unfavorable expansion matching, increased aerodynamic losses, or fluid-specific limitations in multistage operation. Moreover, R365mfc is characterized by a high molecular weight and vapor density, which increase sensitivity to stage-wise pressure distribution and amplify irreversible losses during staged expansion. When the total pressure ratio is divided among multiple stages, these characteristics promote higher entropy generation and cumulative aerodynamic losses, reducing the effective utilization of the available enthalpy drop. In contrast, the single-stage configuration enables a more direct exploitation of the large enthalpy drop associated with R365mfc, leading to comparatively higher net power output and efficiency.

Figure 5 compares the turbine efficiencies obtained for single-stage and multistage configurations across the three working fluids investigated. The results indicate a consistent improvement in efficiency when the expansion is distributed over multiple stages. For R245fa and R123, the multistage turbines achieve efficiencies exceeding 60%, representing an increase of approximately 5–7% relative to their single-stage counterparts. This enhancement can be attributed to the reduction in per-stage pressure ratio, which mitigates aerodynamic losses, shock formation, and excessive entropy generation commonly encountered in single-stage operation. In contrast, the single-stage turbines exhibit lower efficiencies due to higher velocity gradients and partial condensation effects, particularly for dense fluids such as R365mfc. Interestingly, the efficiency gap is most pronounced for R365mfc, highlighting the fluid's sensitivity to expansion characteristics and the advantages of staged expansion in minimizing irreversibilities.

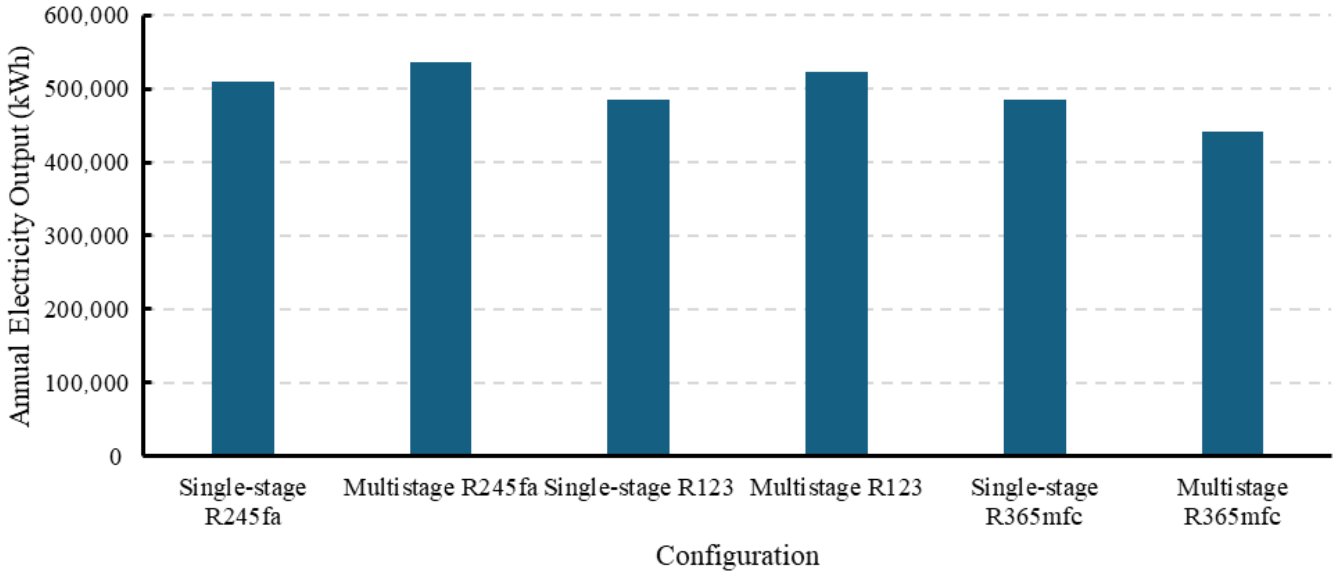


Figure 4. Net turbine power output for single-stage and multistage ORC configurations.

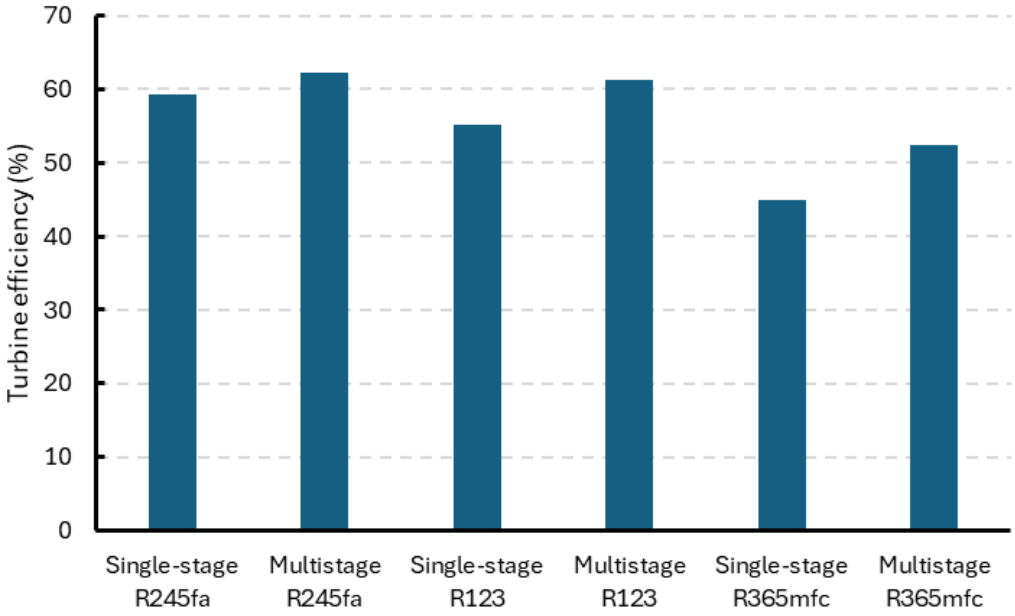


Figure 5. Turbine efficiency for single-stage and multistage ORC configurations.

The variation in thermodynamic performance among the investigated working fluids can be directly attributed to differences in their thermophysical properties. R245fa exhibits superior net power output and turbine efficiency due to its balanced molecular weight and moderate vapor density, which promote favorable expansion characteristics and reduced irreversibility during turbine operation. Its pressure–enthalpy behavior enables efficient energy conversion while limiting excessive velocity gradients and entropy generation, particularly in multistage configurations. R123 benefits from its higher critical temperature, allowing improved thermodynamic matching at elevated heat-source temperatures and sustaining competitive performance under high inlet conditions. In contrast, R365mfc, characterized by a higher molecular weight and vapor density, shows increased sensitivity to expansion matching and irreversible losses, which explains its comparatively lower efficiency and diminished performance gains in multistage operation. These results highlight

the critical role of working-fluid thermophysical properties in governing turbine expansion behavior and overall ORC performance.

3.2. Economic Performance and Capital Recovery

Figure 6 presents the estimated annual revenue for six ORC configurations, calculated at a fixed electricity selling price of 0.10 USD/kWh. As anticipated, the revenue distribution closely reflects the electricity generation results, given the direct proportionality between revenue and net power output. The multistage R245fa system achieves the highest revenue, approaching USD 53,500 per year, indicating the fluid's advantageous thermodynamic characteristics and the efficiency gains associated with multistage expansion. Multistage R123 follows with a comparable revenue level, further confirming the competitiveness of this fluid in advanced turbine arrangements. In contrast, the single-stage cycles of R245fa and R123, while slightly less profitable, still exceed USD 48,000 annually, illustrating the impact of turbine design simplicity on overall financial performance. The lowest revenues are observed for R365mfc-based systems, with the multistage variant performing worst, generating less than USD 45,000 annually. This diminished outcome is most likely linked to suboptimal expansion characteristics and reduced thermal efficiency relative to the other fluids.

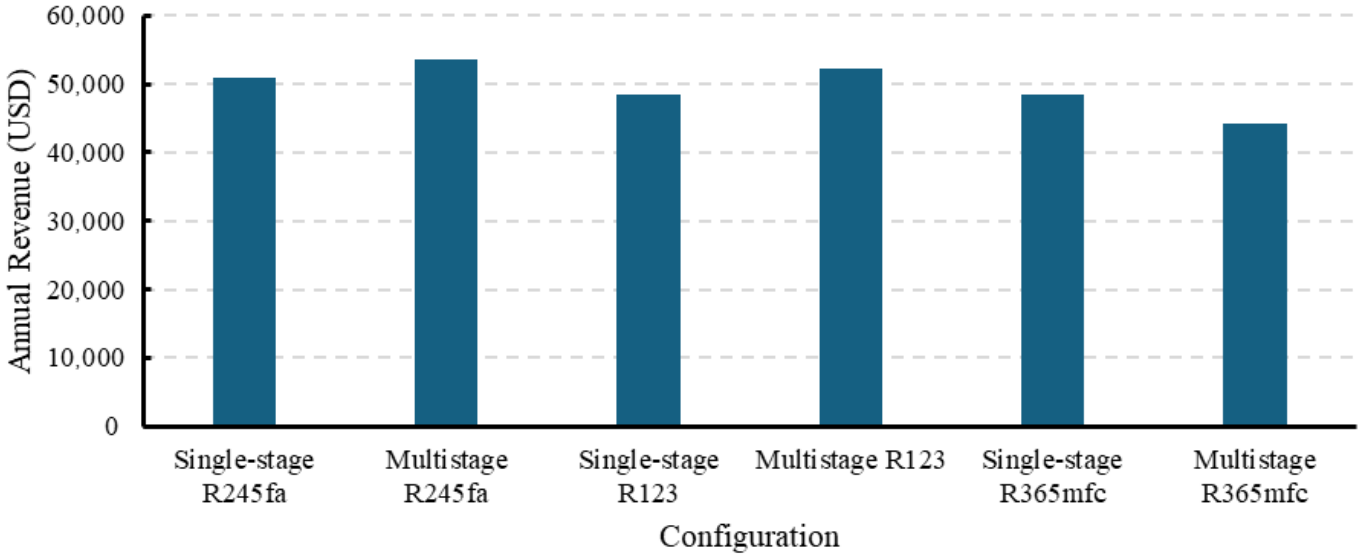


Figure 6. Annual revenue of the system considering different turbine configurations.

Figure 7 compares the annual profit generated by the six different configurations. Interestingly, despite variations in turbine design and working fluid, the annual profit remains within a relatively narrow band across most configurations, ranging from approximately USD 45,000 to just under USD 49,000. The multistage R245fa configuration shows the highest annual profit, followed by the single-stage R245fa. This indicates that, while multistage designs generally incur higher OPEX, the additional revenue they generate can offset those costs when properly matched with a suitable working fluid. Notably, the multistage R365mfc configuration produces the lowest annual profit, under USD 40,000, which reflects both its lower energy conversion efficiency and higher operating costs. The single-stage R365mfc case performs marginally better, likely due to reduced system complexity and maintenance requirements.

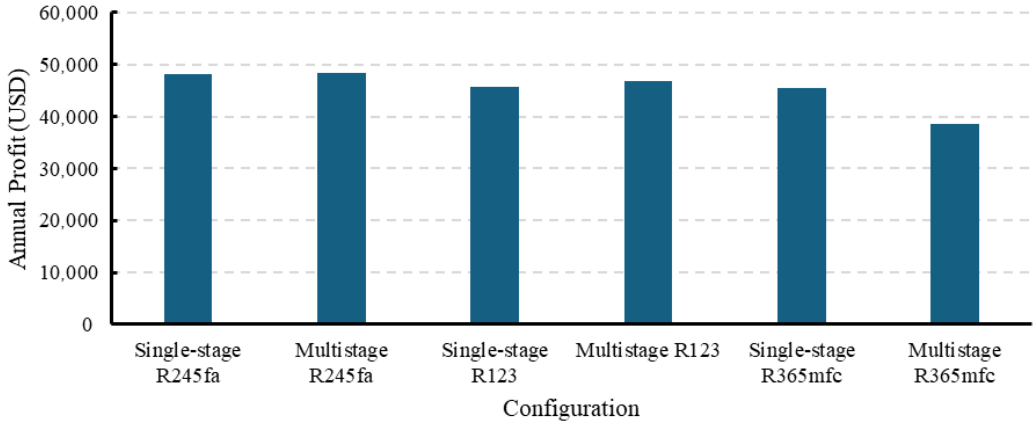


Figure 7. Annual profit of the system considering different turbine configurations.

Figure 8 depicts the economic trade-off between Levelized Cost of Electricity (LCOE) and Net Present Value (NPV) for six ORC configurations, thereby illustrating the combined influence of turbine staging and working fluid selection on system viability. The most desirable designs are in the top-left quadrant of the plot, where low generation costs align with high profitability. Within this framework, the single-stage R245fa configuration emerges as the most favorable option, achieving both the lowest LCOE (~0.021 USD/kWh) and the highest NPV (~USD 463,000). This confirms its status as the most cost-effective solution among the evaluated cases. Multistage R245fa and both R123-based configurations also demonstrate strong performance, providing a favorable balance between economic returns and electricity costs. In contrast, the multistage R365mfc system proves least attractive, exhibiting the highest LCOE (~0.037 USD/kWh) and the lowest NPV (~USD 317,000), indicating that the additional turbine complexity fails to offset its weaker thermodynamic characteristics. Although the single-stage R365mfc design offers marginal improvement, it remains significantly less competitive than R245fa- and R123-based systems. These findings emphasize that while multistage turbines can enhance power output, their economic viability is strongly contingent upon fluid selection and cost–performance optimization.

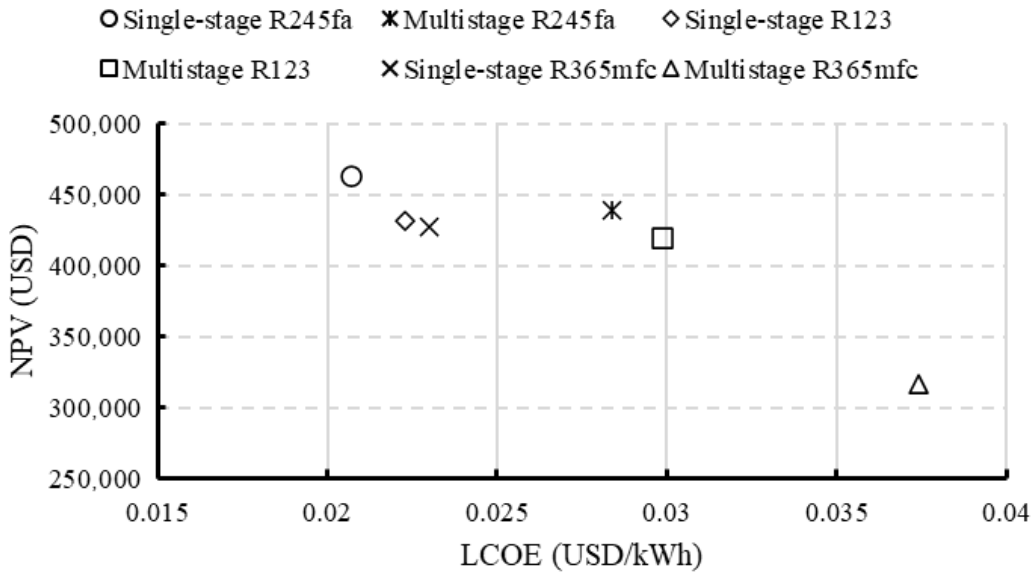


Figure 8. Net Present Value (NPV) versus Levelized Cost of Electricity (LCOE) for different turbine configurations.

The results presented in Figure 8 are verified through consistency with the underlying calculated parameters governing both LCOE and NPV, including annual electricity generation, capital expenditure, and operating costs. Configurations characterized by higher net electricity output and lower specific investment cost, such as the single-stage R245fa system, yield lower LCOE values and higher NPV, whereas systems with increased capital intensity and reduced power output, particularly multistage configurations operating with R365mfc, shift toward higher LCOE and lower NPV. These trends are fully consistent with the annual revenue and profit distributions shown in Figures 5 and 6, as well as the payback-period behavior reported in Figure 8. The agreement among multiple independent economic indicators confirms the correctness and robustness of the calculations underlying Figure 7.

Figure 9 illustrates the payback period for six ORC configurations, indicating the number of years required for each system to recover its initial capital investment through annual operating profits. The results reveal that all configurations achieve financial breakeven within approximately 7.8 to 9.3 years, under the assumption of constant electricity prices and steady annual operating conditions. Among the assessed cases, the single-stage R245fa system demonstrates the most favorable outcome, with a payback period just under 8 years, highlighting its strong balance between capital expenditure and annual profitability. This is followed by the single-stage R123 and single-stage R365mfc systems, both of which recover investment in slightly more than 8 years. By contrast, the multistage R365mfc configuration records the least favorable performance, with a payback period exceeding 9.3 years, indicating that the higher costs associated with the multistage turbine are not adequately offset by the additional energy output.

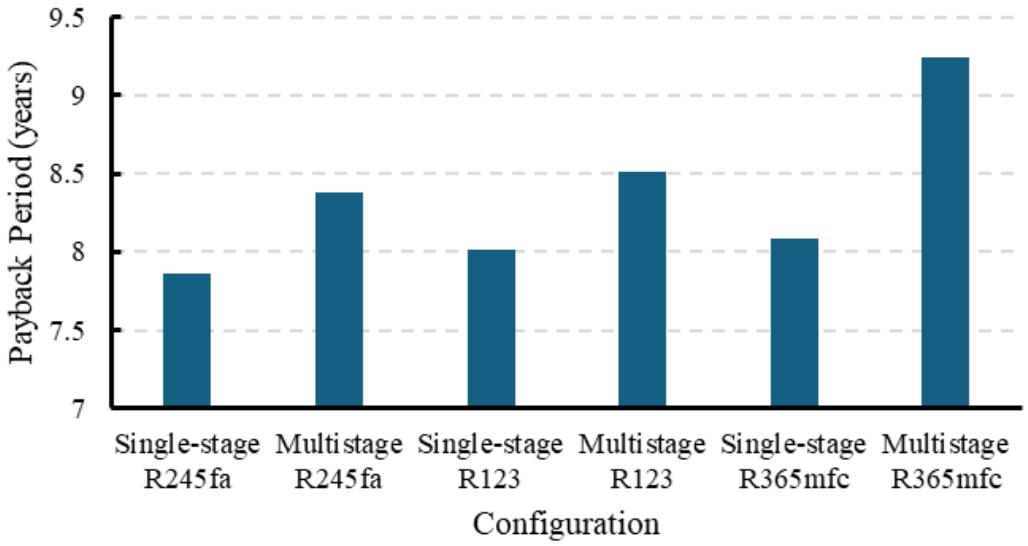


Figure 9. Payback period of the system considering different turbine configurations.

Notably, while multistage turbines typically enhance thermal efficiency and power production, their elevated capital and operating expenses can extend the payback horizon if not paired with high-performing working fluids. This trend is evident in the cases of multistage R123 and multistage R245fa, both of which exhibit longer payback times relative to their single-stage counterparts despite superior energy performance.

3.3. Exergo-Economic Insights

Figure 10 presents the normalized exergy destruction cost for six ORC configurations. This indicator quantifies the share of total system cost attributable to thermodynamic irreversibilities, normalized against a reference case, the single-stage R245fa configuration,

assigned a baseline value of 1.0. Lower values; therefore, denote more energy-efficient and cost-effective designs from an exergo-economic perspective. The results show that multistage turbines substantially reduce exergy destruction costs, with normalized values falling below 0.2 for all three working fluids. Among these, the multistage R365mfc system achieves the lowest exergy destruction, closely followed by multistage R123 and multistage R245fa. These improvements can be attributed to the superior thermodynamic performance of multistage expansion, which minimizes entropy generation and ensures better matching between pressure ratios and working-fluid characteristics. In contrast, single-stage turbines display markedly higher normalized exergy destruction costs. Both the single-stage R123 and single-stage R365mfc systems exceed 0.85, indicating that their simpler expansion processes impose greater irreversibilities, particularly when paired with fluids exhibiting non-ideal expansion behavior. Although the single-stage R245fa configuration performs strongly in terms of overall economic indicators, it remains the highest on this scale, as it serves as the normalization reference.

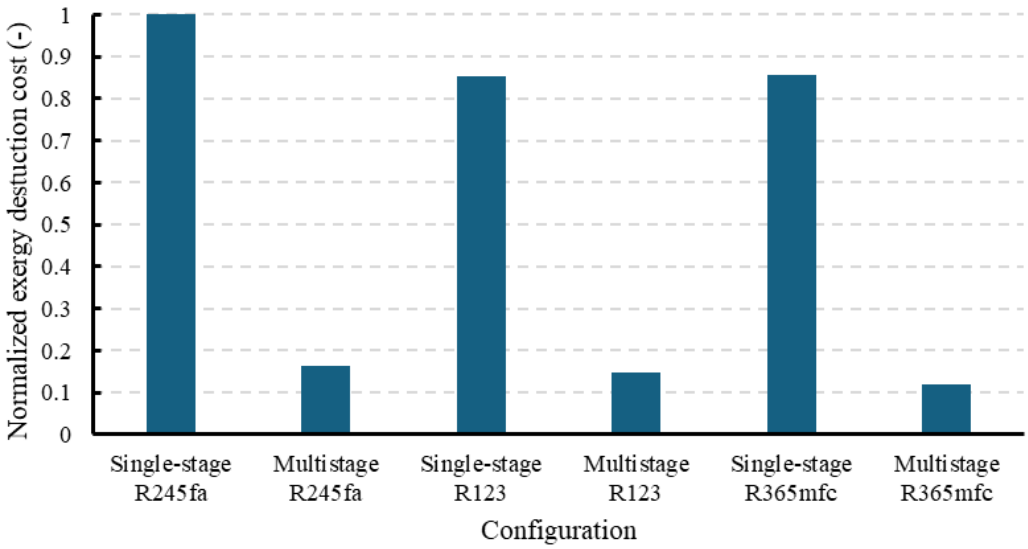


Figure 10. Normalized exergy destruction cost of the system considering different turbine configurations.

Figure 11 illustrates the unit exergy cost for six ORC configurations. The unit exergy cost provides an exergo-economic measure of the financial impact of thermodynamic irreversibilities, with lower values signifying more efficient and cost-effective energy conversion. The results show that multistage configurations consistently outperform their single-stage counterparts for all fluids. Among these, the multistage R365mfc system achieves the lowest unit exergy cost, followed by multistage R123 and multistage R245fa. Reductions on the order of 80–90% compared with the corresponding single-stage systems highlight the substantial exergo-economic advantages of distributing expansion across multiple stages. In contrast, single-stage systems, particularly those operating with R123 and R365mfc, display unit exergy costs above 0.85, reflecting higher penalties from exergy destruction. The single-stage R245fa configuration, defined as the normalization baseline (value = 1.0), reinforces this comparison. Overall, these results emphasize the pivotal role of turbine design in minimizing the economic consequences of irreversibilities and strongly support the adoption of multistage turbines in ORC applications where high exergetic efficiency and low operating costs are prioritized.

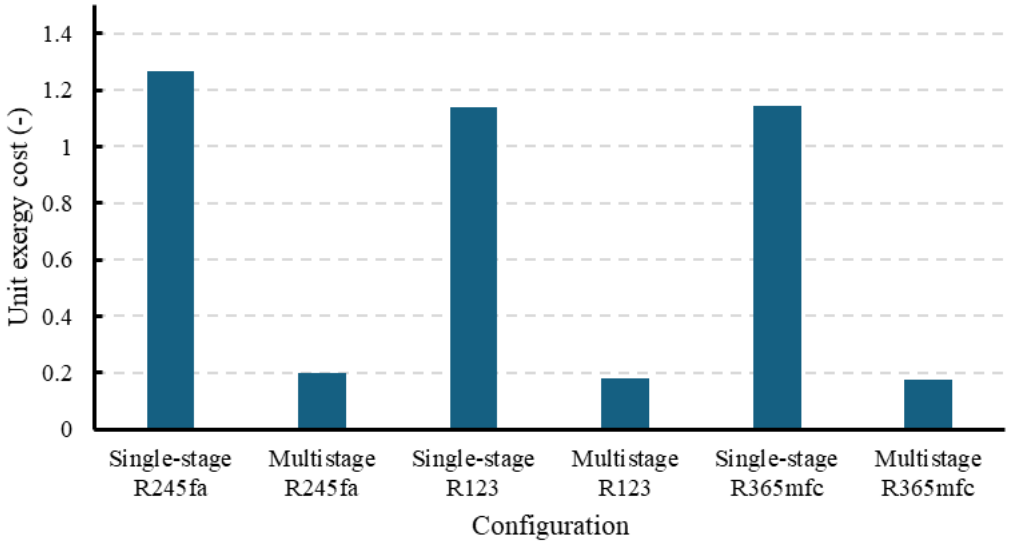


Figure 11. Unit exergy destruction cost per kWh of electricity generated.

3.4. Parametric Considerations and Sensitivity Analysis

Figure 12 illustrates the effect of heat source temperature on thermal efficiency and annual electricity output for single-stage and multistage ORC systems. As anticipated, both indicators increase markedly with higher source temperatures, indicating the thermodynamic benefits of utilizing elevated-temperature heat streams. Across the entire range (120 °C to 200 °C), the multistage configuration consistently outperforms the single-stage design due to superior expansion efficiency and improved alignment with the working fluid's pressure–enthalpy behavior.

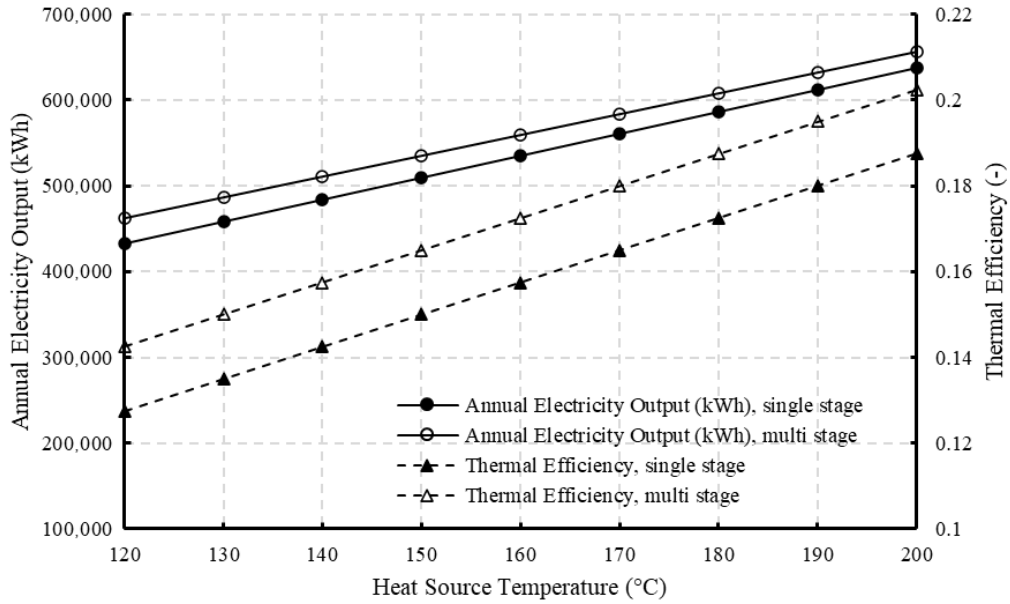


Figure 12. Annual electricity generated for different heat source temperatures considering different turbine configurations, using R245fa.

For thermal efficiency, the multistage system improves from approximately 13% at 120 °C to above 21% at 200 °C, compared with a rise from roughly 11% to 19% for the single-stage case. This persistent ~2% gap reflects reduced exergy destruction and more effective pressure utilization in the multistage turbine. The efficiency advantage directly translates into higher electricity generation (left axis), with the multistage cycle producing

40,000–50,000 kWh more annually at all temperature levels. For instance, at 150 °C, the single-stage system yields just under 500,000 kWh per year, whereas the multistage system exceeds 530,000 kWh.

These findings confirm that higher source temperatures and multistage turbine integration are critical enablers of enhanced ORC performance. They further highlight the importance of thermal integration strategies and turbine design optimization when exploiting low- to medium-grade heat sources in industrial and renewable applications.

Figure 13 depicts the influence of heat source temperature on the LCOE and NPV for both single-stage and multistage ORC systems. The left y-axis corresponds to LCOE (USD/kWh), while the right y-axis represents NPV (USD). The results confirm that increasing heat source temperature markedly improves economic performance in both configurations, primarily due to enhanced thermal conversion efficiency and higher annual power generation. For both systems, LCOE decreases steadily with temperature; however, the multistage cycle initially incurs higher LCOE values owing to its greater capital and operational costs. The cost trajectories intersect at approximately 155–160 °C, above which the multistage system becomes more competitive on a per-kWh basis. With respect to profitability, both configurations exhibit steadily increasing NPV as temperature rises. Beyond 150 °C, the multistage system consistently outperforms the single-stage, demonstrating superior long-term financial viability despite higher initial investment requirements. At 200 °C, the NPV of the multistage system approaches USD 600,000, exceeding that of the single-stage design by nearly USD 50,000. Collectively, these results indicate that the economic benefits of multistage expansion become increasingly pronounced at elevated source temperatures, reinforcing its suitability for high-grade waste heat recovery and geothermal energy applications.

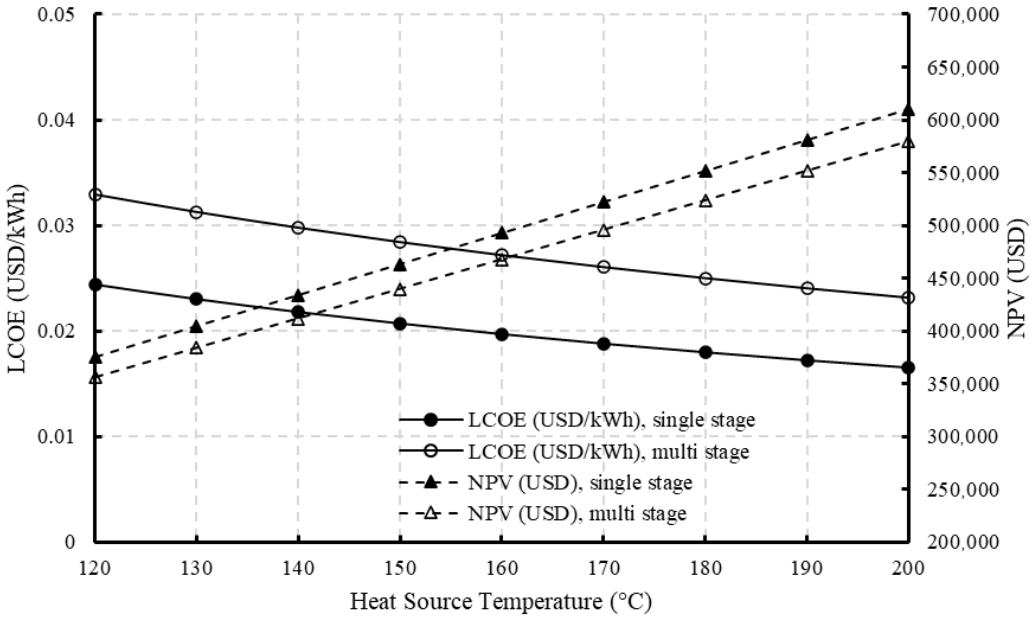


Figure 13. Effects of the heat source temperature on the economic aspects for different turbine configurations, using R245fa.

Figure 14 illustrates the variation in the payback period as a function of heat-source temperature for single-stage and multistage ORC configurations. As anticipated, higher source temperatures consistently reduce payback time in both systems, owing to improved thermal efficiency and increased annual electricity generation that enhance revenue and accelerate investment recovery. Across the entire range, the single-stage design maintains a shorter payback period, reflecting its lower capital and operational costs.

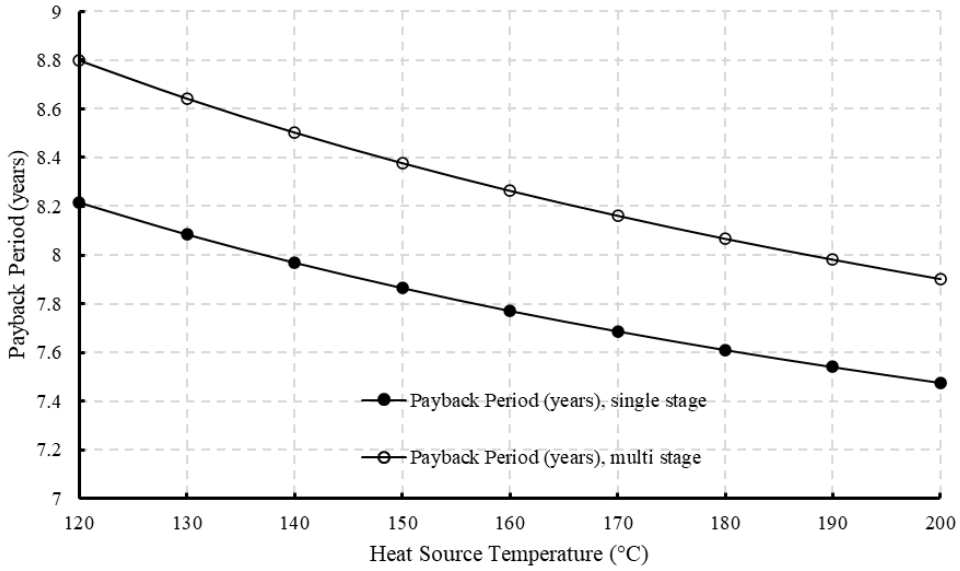


Figure 14. Effects of the heat source temperature on the system payback period for different turbine configurations, using R245fa.

At lower temperatures (e.g., 120 °C), the disparity between the two designs is more evident, with the multistage system requiring roughly 8.8 years compared to 8.2 years for the single-stage configuration. As the source temperature approaches 200 °C; however, the difference diminishes, and both systems achieve payback in under 8 years, with the multistage system approaching parity. This convergence indicates that the economic penalty of multistage systems at low temperatures is offset at higher temperatures, where enhanced thermodynamic performance leads to greater annual profitability.

Overall, the results highlight that while both systems benefit from elevated heat-source temperatures, the relative attractiveness of multistage turbines improves significantly above 170 °C, making them particularly suited for high-grade waste-heat recovery and geothermal energy utilization.

4. Conclusions

Harnessing waste heat represented a critical opportunity for improving energy efficiency and reducing fuel consumption in maritime and stationary power-generation systems. Large quantities of recoverable thermal energy were routinely discharged to the environment, and their effective utilization was increasingly important for achieving cost-effective decarbonization. Within this context, this study conducted a comprehensive thermodynamic, economic, and exergo-economic assessment of Organic Rankine Cycle systems employing single-stage and multistage radial turbine configurations.

Six ORC layouts were evaluated using R245fa, R123, and R365mfc as working fluids. The results showed that multistage turbines enhanced thermal efficiency and net power output while substantially reducing exergy destruction costs. These performance improvements were accompanied by higher capital and operating expenditures, which in many cases extended the payback period. Multistage configurations improved turbine efficiency by approximately 5–7% and increased annual electricity generation beyond 530,000 kWh for R245fa, while reducing exergy destruction costs by more than 80%. From an economic perspective, the multistage system operating with R365mfc exhibited the least favorable performance, with an LCOE of approximately 0.037 USD/kWh and a payback period exceeding nine years.

By contrast, the single-stage ORC operating with R245fa delivered the most balanced outcome in terms of technical performance and economic feasibility. This configura-

tion achieved the lowest LCOE (around 0.021 USD/kWh), the highest net present value (approximately 463,000 USD), and the shortest payback period, remaining below eight years. Overall, the findings indicated that multistage turbine arrangements were most suitable for high-temperature heat sources above 170 °C, whereas for typical waste heat recovery conditions, a single-stage R245fa-based ORC constituted the most economically attractive configuration.

Although the present study provides a comprehensive system-level thermodynamic, economic, and exergo-economic comparison of ORC turbine configurations, several limitations should be acknowledged. The analysis is conducted under steady-state conditions and adopts system-level assumptions, such as negligible pressure losses, which are appropriate for configuration screening but do not capture detailed component-level aerodynamic and mechanical phenomena. In addition, ship-specific installation aspects, including motion-induced effects (sway and pitch), space and weight constraints, and detailed mechanical layout considerations, are not explicitly modeled. Future research will focus on extending the present framework to include motion-aware performance analysis, layout- and volume-constrained optimization for shipboard ORC systems, and detailed aerodynamic and mechanical modeling of multistage turbines.

Author Contributions: Conceptualization, S.A. and F.A.; methodology, S.A., M.H.A. and M.A.; software, A.P. and N.A.; validation, F.A., S.A. and M.A.; formal analysis, M.H.A. and S.A.; investigation, F.A.; resources, F.A.; data curation, A.P. and N.A.; writing—original draft preparation, S.A.; writing—review and editing, all authors.; visualization, N.A.; supervision, F.A.; project administration, F.A.; funding acquisition, F.A. All authors have read and agreed to the published version of the manuscript.

Funding: This research has been funded by the Scientific Research Deanship at the University of Ha'il—Saudi Arabia through project number [RG-25 037].

Data Availability Statement: The original contributions presented in this study are included in the article. Further inquiries can be directed to the corresponding author.

Conflicts of Interest: The authors declare no conflicts of interest.

Abbreviations

The following abbreviations are used in this manuscript:

Symbol	Description	Unit
$\dot{m}_{wf}$	Mass flow rate of working fluid	kg/s
h	Specific enthalpy	kJ/kg
$\dot{Q}_{evap}$	Heat absorbed from the heat source (evaporator)	kW
$\dot{Q}_{cond}$	Heat rejected in the condenser	kW
$\dot{W}_{turb}$	Turbine power output	kW
$\dot{W}_{pump}$	Pump power input	kW
η_{th}	Thermal efficiency of ORC system	– or %-
CAPEX	Capital expenditure	USD
OPEX	Operating expenditure	USD/year
NPV	Net present value	USD
LCOE	Levelized cost of electricity	USD/kWh
$Payback$	Payback period	years
E_{annual}	Annual electricity generation	kWh/year
P_{annual}	Electricity selling price	USD/kWh
α	OPEX-to-CAPEX ratio	–
r	Discount rate	%

References

1. Li, Z.; Wang, K.; Liang, H.; Wang, Y.; Ma, R.; Cao, J.; Huang, L. Marine alternative fuels for shipping decarbonization: Technologies, applications and challenges. *Energy Convers. Manag.* **2025**, *329*, 119641. [CrossRef]
2. Zhu, S.; Feng, J.; Tang, Y.; Bai, S.; Deng, K. Influence of ambient conditions on the marine two-stroke engine integrated with a bottoming Rankine cycle system: Energy and exergy analyses. *Appl. Therm. Eng.* **2023**, *219*, 119601. [CrossRef]
3. Kareem, A.F.; Akroot, A.; Wahhab, H.A.A.; Talal, W.; Ghazal, R.M.; Alfaris, A. Exergo–Economic and Parametric Analysis of Waste Heat Recovery from Taji Gas Turbines Power Plant Using Rankine Cycle and Organic Rankine Cycle. *Sustainability* **2023**, *15*, 9376. [CrossRef]
4. Alshammari, F.; Alatawi, I.; Alshammari, A.S. Impact of turbine characteristics on low temperature organic Rankine cycles operating with zeotropic and azeotropic mixtures. *Case Stud. Therm. Eng.* **2024**, *59*, 104463. [CrossRef]
5. Chowdhury, A.S.; Ehsan, M.M. A Critical Overview of Working Fluids in Organic Rankine, Supercritical Rankine, and Supercritical Brayton Cycles Under Various Heat Grade Sources. *Int. J. Thermofluids* **2023**, *20*, 100426. [CrossRef]
6. Baniam, M.; Yari, M.; Mehr, A.S. Optimization waste heat recovery and power generation for industrial sustainability: A comparative study of supercritical CO2 Brayton, organic Rankine, and inverted Brayton cycles with synthesis natural gas as heat source. *Therm. Sci. Eng. Prog.* **2024**, *47*, 102303. [CrossRef]
7. Alharbi, M.; Alshammari, F. Numerical Evaluation of Equation of State Sensitivity in Energy Conversion Systems. *Mathematics* **2025**, *13*, 1826. [CrossRef]
8. Ventura, C.A.M.; Jacobs, P.A.; Rowlands, A.S.; Petrie-Repar, P.; Sauret, E. Preliminary design and performance estimation of radial inflow turbines: An automated approach. *J. Fluids Eng.* **2012**, *134*, 031102. [CrossRef]
9. Agromayor, R.; Nord, L.O. Preliminary Design and Optimization of Axial Turbines Accounting for Diffuser Performance. *Int. J. Turbomach. Propuls. Power* **2019**, *4*, 32. [CrossRef]
10. Stanitz, J.D. Some Theoretical Aerodynamic Investigations of Impellers in Radial-and Mixed-Flow Centrifugal Compressors. *Trans. Am. Soc. Mech. Eng.* **1952**, *74*, 473–497. [CrossRef]
11. Xu, G.; Zhao, G.; Quan, Y.; Liang, R.; Li, T.; Dong, B.; Fu, J. Design and optimization of a radial-axial two-stage coaxial turbine for high-temperature supercritical organic Rankine cycle. *Appl. Therm. Eng.* **2023**, *227*, 120365. [CrossRef]
12. Peng, N.; Wang, E.; Zhang, H. Preliminary Design of an Axial-Flow Turbine for Small-Scale Supercritical Organic Rankine Cycle. *Energies* **2021**, *14*, 5277. [CrossRef]
13. Alshammari, F.; Alharbi, M.; Pesyridis, A. Improving heat recovery: A unified one-dimensional radial turbine model for CO_2 reduction and efficiency gains in automotive organic Rankine cycles. *Appl. Therm. Eng.* **2025**, *267*, 125816. [CrossRef]
14. Zheng, Q.; Sun, L.; Chang, S.; Xing, H. Techno-Economic Analysis of Multi-Purpose Heavy-Lift Vessels Using Methanol as Fuel. *J. Mar. Sci. Eng.* **2025**, *13*, 1234. [CrossRef]
15. Zhao, S.; Pazouki, K.; Norman, R. Performance Evaluation of Combined Wind-Assisted Propulsion and Organic Rankine Cycle Systems in Ships. *J. Mar. Sci. Eng.* **2025**, *13*, 1287. [CrossRef]
16. Xing, H.; Chang, S.; Ma, R.; Wang, K. EU MRV Data-Based Review of the Ship Energy Efficiency Framework. *J. Mar. Sci. Eng.* **2025**, *13*, 1437. [CrossRef]
17. Feng, J.; Gu, Y.; Han, S.; Zhao, X.; Tang, Y.; Zhu, S.; Yuan, H.; Wang, G. Design of Organic Rankine Cycle Recovering Multi-Grade Waste Heat from a Two-Stroke Marine Engine. *J. Mar. Sci. Eng.* **2025**, *13*, 1679. [CrossRef]
18. Kindra, V.; Maksimov, I.; Zuikin, R.; Malenkov, A.; Rogalev, A. Thermodynamic Analysis of Combined-Cycle Power Plants Incorporating an Organic Rankine Cycle and Supplementary Burners. *Energies* **2025**, *18*, 5909. [CrossRef]
19. Lu, B.; Liu, Y.; Zhai, X.; Zhang, L.; Chen, Y. Design and Experimental Study of 50 kW Ocean Thermal Energy Conversion Test Platform Based on Organic Rankine Cycle. *J. Mar. Sci. Eng.* **2024**, *12*, 463. [CrossRef]
20. Elrhoul, D.; Naveiro, M.; Gómez, M.R. Thermo-Economic Comparison between Three Different Electrolysis Technologies Powered by a Conventional Organic Rankine Cycle for the Green Hydrogen Production Onboard Liquefied Natural Gas Carriers. *J. Mar. Sci. Eng.* **2024**, *12*, 1287. [CrossRef]
21. Jiménez-García, J.C.; Ruiz, A.; Pacheco-Reyes, A.; Rivera, W. A Comprehensive Review of Organic Rankine Cycles. *Processes* **2023**, *11*, 1982. [CrossRef]
22. Lee, H.; Jung, J.; Kim, Y.; Kim, S.; Jeon, H. Comparative Analysis of Mechanical and Hybrid Propulsion Systems for Buoy Maintenance Vessel Based on Real-Sea Operational Data. *J. Mar. Sci. Eng.* **2025**, *13*, 2279. [CrossRef]
23. Escalante, E.S.R.; Balestieri, J.A.P.; de Carvalho, J.A. The organic Rankine cycle: A promising technology for electricity generation and thermal pollution mitigation. *Energy* **2022**, *247*, 123405. [CrossRef]
24. Astolfi, M.; Romano, M.C.; Bombarda, P.; Macchi, E. Binary ORC (organic Rankine cycles) power plants for the exploitation of medium–low temperature geothermal sources—Part A: Thermodynamic optimization. *Energy* **2014**, *66*, 423–434. [CrossRef]
25. Fan, M.; Zhao, Y.; Liu, M.; Yan, J. Feedwater control enhancement of thermal power plants with cascade Rankine cycle during peak shaving: Restrictions and control strategy optimization. *Energy* **2025**, *338*, 138955. [CrossRef]

26. Latz, G.; Andersson, S.; Munch, K. Selecting an Expansion Machine for Vehicle Waste-Heat Recovery Systems Based on the Rankine Cycle. In *Proceedings of the SAE 2013 World Congress & Exhibition, Detroit, MI, USA, 16–18 April 2013*; SAE International: Warrendale, PA, USA, 2013; Volume 1, pp. 1–15. [CrossRef]
27. Lemmon, E.; Huber, M.; McLinden, M. *NIST Standard Reference Database 23: Reference Fluid Thermodynamic and Transport Properties-REFPROP, Version 9.0*; National Institute of Standards and Technology, Standard Reference Data Program: Gaithersburg, MA, USA, 2010.
28. Alshammari, F.; Alharbi, M.; Alharbi, S. Enhanced thermal efficiency in off-highway vehicles using a reheat organic Rankine cycle with a two-stage radial turbine and wet fluids. *Case Stud. Therm. Eng.* **2025**, *71*, 106223. [CrossRef]
29. Martire, R.N.M.; Erguvan, M.; Amini, S. Integrated solar organic Rankine Cycle and Direct Air Capture System for sustainable automotive manufacturing plants. *Energy Convers. Manag. X* **2025**, *28*, 101382. [CrossRef]
30. García-Afonso, Ó.; Delgado-Torres, A.M.; González-Díaz, B. Potential of Organic Rankine Cycle for waste heat recovery from piston engine-based power plants in isolated power systems. *Appl. Therm. Eng.* **2022**, *203*, 117815. [CrossRef]

Disclaimer/Publisher's Note: The statements, opinions and data contained in all publications are solely those of the individual author(s) and contributor(s) and not of MDPI and/or the editor(s). MDPI and/or the editor(s) disclaim responsibility for any injury to people or property resulting from any ideas, methods, instructions or products referred to in the content.